Tunable Spoof Surface Plasmons Bulleye Antenna

Zhuo Li, Chen Chen, Liangliang Liu, Jia Xu, Yunhe Sun, Bingzheng Xu, Hengyi Sun, Xinlei Chen & Changqing Gu

Plasmonics

ISSN 1557-1955

Plasmonics
DOI 10.1007/s11468-017-0562-9

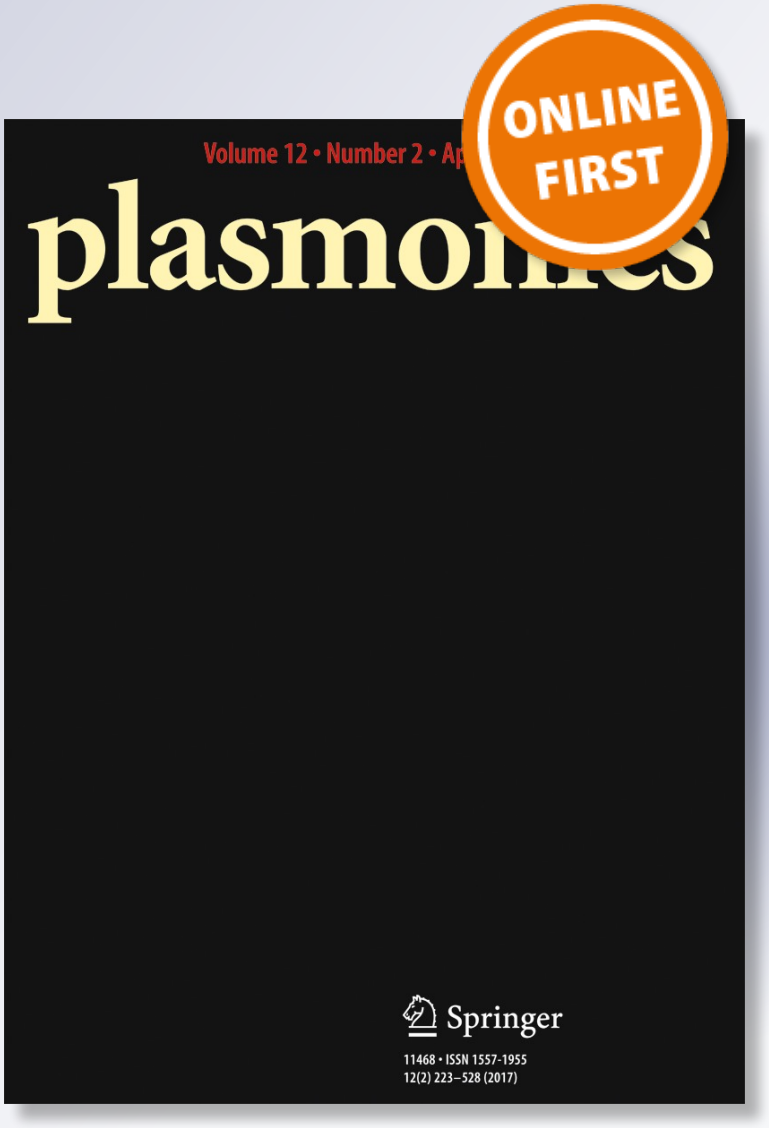

Springer

Plasmonics
DOI 10.1007/s11468-017-0562-9

Tunable Spoof Surface Plasmons Bulleye Antenna

Zhuo Li[1,2] · Chen Chen[1] · Liangliang Liu[1] · Jia Xu[1] · Yunhe Sun[1] · Bingzheng Xu[1] · Hengyi Sun[1] · Xinlei Chen[1] · Changqing Gu[1]

Received: 23 November 2016 / Accepted: 2 March 2017

Abstract A tunable spoof surface plasmons antenna using sinusoidally modulated corrugated reactance surface based on a bulleye structure is proposed in this paper. The designed antenna is made of concentric metallic grooves etched on a metal plate, the depth of which is of sinusoidal periodic variation in the radial direction. This makes it possible that highly confined spoof surface plasmons along corrugated surface can be converted to radiation modes. The proposed bulleye antenna can work from 25.8 to 33 GHz and a bandwidth of 7.2 GHz and its main lobe can be directed at 30° from the vertical direction at 30 GHz. This antenna has a maximum gain of 15 dB and its main lobe can scan from 14° to 58° by tuning the frequency from 28 to 32 GHz.

Keywords Spoof plasmons · Spatial waves · Conversion · Bulleye structure · Sinusoidal modulation

Introduction

Surface plasmon polaritons (SPPs) are a prominent class of surface waves excited along metallic corrugated surfaces at the interface between metal and dielectric in optical frequencies, which have substantial applications in subwavelength optics, low-loss transmission and photonic devices and play a pivotal role in the advancement of modern plasmonics or nanophotonics [1–5]. However, metals are not characterized by negative dielectric permittivity and behave as perfect electric conductor in microwave and terahertz(THz) regimes that SPPs may not be excited along their surfaces. To inherit most of the amazing features of SPPs to lower frequencies, researchers have proposed some solutions by etching metal surfaces with periodic grooves or holes to support similar high-confined surface waves, named spoof surface plasmon polaritons(SSPPs) [6–9]. Thereafter, a series of efforts have been conducted to put the SSPPs into practical uses by constructing smooth bridges between traditional transmission lines and SSPPs waveguide [10, 11], the development of SSPPs filters [12, 13], waves splitters [14], amplifiers, and other passive and active functional devices in the microwave and terahertz frequencies.

Mode conversion from guided waves to SSPPs has been widely studied and SSPPs devices has been developed as well. However, spoof surface plasmons antenna, which is capable of converting SSPPs to spatial waves has not been fully studied. It is not easy to realize direct radiations of SSPPs because it is characterized by strong field confinement with the propagation wave number being greater than that of free space while a leaky wave structure requires a smaller wave number [15]. However, this does not mean that it is impossible to realize SSPPs antenna. An efficient method to convert SSPPs to radiated spatial waves directly using metallic corrugated strip with gradient grooves and flaring structure was recently proposed in [16], in which the gradient grooves are used to overcome the big mismatch of wave number between SSPPs and the radiated spatial waves while the flaring structure provides impedance matching in a wide frequency band. A SSPPs emitter composed of

✉ Zhuo Li
lizhuo@nuaa.edu.cn

[1] Key Laboratory of Radar Imaging and Microwave Photonics, Ministry of Education, College of Electronic and Information Engineering, Nanjing University of Aeronautics and Astronautics, Nanjing, 211106, China

[2] State Key Laboratory of Millimeter Waves, Southeast University, Nanjing, 210096, China

Published online: 16 March 2017

ultrathin corrugated metallic strips together with the phase-gradient metasurface on it was proposed in [17], providing a simple route to efficiently convert SSPPs to radiating waves and exhibiting directional radiation properties.

There also exists another systematic approach to realize efficient coupling from SSPPs to free space radiating waves, which is based on the fact that surface waves can be converted to a leaky mode if a periodic perturbation is introduced along the guiding structure [15]. More specifically, reactance surfaces can support leaky wave modes if a sinusoidally modulated reactance surface (SMRS) perturbation is introduced [18]. Since the corrugated surface that supports SSPPs is actually a reactance surface, leaky wave structures based on SSPPs and SMRS have been used for SSPPs antenna design. Both planar and cylindrical structures were numerically demonstrated to be able to convert guided SSPPs to radiating modes by introducing sinusoidally modulated corrugated reactance surfaces (SMRS) [19]. An omnidirectional antenna utilizing periodically modulated double-edge corrugated metallic strips was proposed in [20], in which the depths of grooves were periodically modulated for mode conversion. In addition, THz bessel beamforming based on a leaky plasmonic waveguide composed of concentric metallic grooves with a subwavelength spacing was experimentally demonstrated in [21]. Such a structure is usually called a bulleye. However, there remains a relatively blank area to convert SSPPs to spatial waves using SMRS based on bulleye structures so far.

In this work, we intend to design an antenna that can realize mode conversion from SSPPs to radiated spatial waves based on the bulleye structure, which is made of concentric metallic grooves etched on a metal plate as shown in Fig. 2, the depth of which is of sinusoidal periodic variations in the radial direction. The main lobe of the proposed bulleye antenna can be exactly directed at the angle that we design in theory and the radiation pattern is omnidirectional in azimuth plane. Furthermore, the designed antenna has a wide operating bandwidth of 7.2 GHz and beam scanning function by tuning the working frequency. The radiation efficiency is more than 90% in the whole operating band, exhibiting great potentials in SSPPs antenna system. Omnidirectional radiation characteristic in the azimuth plane can be realized with the bulleye antenna, which cannot be realized with planar or cylindrical corrugated surface proposed in [19]. In addition, we extends the applications of the bulleye structure to realize directional radiations of SSPPs via sinusoidally modulated surface.

Theoretical Analysis

In this section, design principles of the proposed SMRS bulleye antenna is presented in detail based on the fact that any surface wave can be converted to a leaky wave if a periodic perturbation is introduced along the guiding surface. Since SSPPs are exactly surface modes propagating along corrugated surfaces and are characterized by a real valued wave number $k > k_0$, where k_0 is the free space wave number. Therefore, if we introduce a periodic reactance perturbation of period p, a modified wave number k_{modi} can be expressed as [22]

$$k_{modi} = k_n - j\alpha \tag{1}$$

according to the Floquet theory. $k_n = k+2\pi n/p$ is the real part of the modified wave number and only when its value is smaller than that of free space ($k+2\pi n/p < k_0$) the surface wave can be converted to radiating modes. n is an integer number indicating the order of the corresponding Floquet mode and the n=-1 mode represents the leaky wave mode in general. Hence, reactance surfaces can sustain leaky wave when periodic reactance perturbation is introduced to modulate the propagation wave number less than the free space wave number.

The elevation angle θ of the main radiation lobe can be calculated by

$$k_0 sin\theta = k - 2\pi/p. \tag{2}$$

If the operating frequency f, the SMRS period p, and the desired radiation angle θ are given, we can calculate the quantitative relation between k and k_0 and obtain the depth of grooves l corresponding to a mean or un-modulated impedance value Z_u around which the impedance value of the corrugated surface fluctuates sinusoidally according to the dispersion relation. Depending on the period of the modulation, one or more radiating spatial harmonics can be excited by the modulated surface and the input impedance of the corrugated surface can be given by

$$Z(\rho) = jZ_u[1 + Mcos(2\pi\rho/p)], \tag{3}$$

where M denotes the modulation factor which in principle can be any value lower than one and can determine the beamwidth of the main radiation lobe.

Considering that the wave number along the radial direction of the bulleye structure have the same expression as that along a planar metallic corrugated structure [23]

$$k_\rho = k_0\sqrt{1 + tan^2 k_0 d}, \tag{4}$$

we can utilize the formula of planar corrugated surface to simplify the design of leaky wave antenna based on the bulleye structure. The schematic diagram of the planar corrugated surface is shown in Fig. 1, which is just the radial cross section profile of the designed bulleye antenna. Geometric parameters d, g, and l marked in Fig. 1 denote the period, width and depth of the grooves respectively.

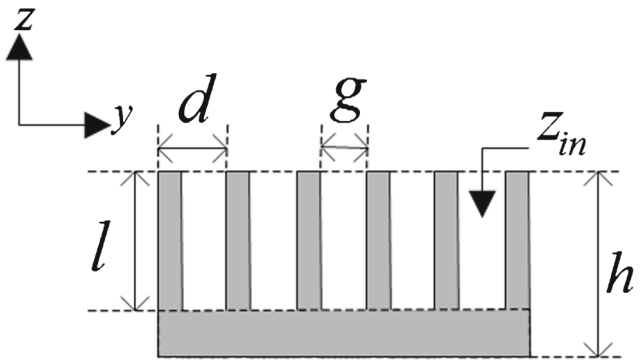

Fig. 1 Profile of the planar corrugated surface. Wave guidance is assumed along the y-direction

The planar corrugated surface shown in Fig. 1 is equivalent to a short circuited TEM transmission line model. Hence the input impedance can be expressed as [23]

$$Z_{in} = jZ_0(g/d)tan(k_0 l). \tag{5}$$

From the above expression, we can calculate the corresponding depth for any given input impedance. It is obvious that there should be a continuous sinusoidal distribution of the impedance values within a SMRS period p in Eq. 2. However, the varying impedance values of a corrugated surface can be represented only at a finite number of discrete spatial points. After some numerical experimentation, it was concluded that 15 sub-unit-cells in one period are sufficient to represent the SMRS variation accurately [19].Thus, we can evaluate the impedance from Eq. 2 at the sequence of points: $\rho_m = (p/15)m$, with m = 0:1:14. These impedance values are then mapped to a sequence of the depth of grooves according to Eq. 5. We should note that the upper frequency for which the corrugated surface can support SSPPs corresponds to the λ/4 resonance of the groove. Thus, all these calculated depth of grooves should be smaller than the λ/4 resonance of the corrugation.

Design and Simulation

The bulleye antenna is composed of 10 SMRS periods and each sinusoidal period p = 9 mm consists of 15 concentric circular grooves with period d = 0.6 mm, width g = 0.4 mm, and a sinusoidally modulated depth l etched on a metal plate with the thickness h = 4 mm as shown in Fig. 2. Moreover, the end of the metal plate is modified with an marginal circle to reduce the reflection caused by abrupt ending with big impedance mismatch. The corrugated surface is excited in the center from the backside of the metal plate by a monopole. The diameter of the monopole and the outer conductor of the coaxial line are set as $2r$ = 2 mm and $2R$ = 4.6 mm to achieve 50 Ω input impedance. In this design, we set the operating frequency f = 30 GHz and the extended length of monopole from the metallic surface z = 2.5 mm, which equals a quarter of the operating wavelength. In addition, the desired direction of the main radiation lobe is set as $\theta = 30°$.

In accordance with the above given parameters, the propagation constant along the corrugated surface can be calculated from Eq. 2 with the relation of k = 1.61 k_0, which corresponds to the depth of l = 1.7 mm as shown in Fig. 3. Then, by substituting l into Eq. 5, the mean impedance value $Z_u = 1.21Z_0$ around which the impedance value of the corrugated surface fluctuates sinusoidally will be obtained. Here, we set the modulation factor M to 0.3 and a set of impedance values can be calculated at the sequence of points: $\rho_m = (p/15)m$, with m = 0:1:14 depending on Eq. 3. These impedance values are eventually mapped to a sequence of depth of grooves by Eq. 5 as follows: [1.58629, 1.50062, 1.44762, 1.44762, 1.50062, 1.58629, 1.67841, 1.75812, 1.81665, 1.85167, 1.86325, 1.85167, 1.81665, 1.75812, 1.67841]×1 mm.

To confirm the radiation performance of the above designed SMRS bulleye antenna, we conduct numerical simulations using the commercial software CST Microwave Studio and set open (add space) boundary conditions for all six boundaries. The structure shown in Fig. 2 is modeled with PEC and the overall size including the marginal circle is L = 120 mm. The monopole is excited with a TEM mode using a coaxial waveguide port. The radiating performance of the proposed structure is describe as follows.

The designed SSPPs antenna has a wide operating bandwidth of 7.2 GHz covering from 25.8 to 33 GHz with the return loss less than −10 dB, which can be seen from the reflection coefficient S_{11} plotted in Fig. 4. Moreover, Fig. 4 reports the S_{11} performance of the non-SMRS bulleye antenna for comparison which has the same size with the proposed SMRS antenna except that the depth of grooves remains unchanged. Here, we set the constant depth l = 1.7 mm to the mean impedance value of the SMRS antenna. It is apparent that the reflection performance is well improved when sinusoidal modulation is introduced. Figure 5 shows the simulated far-field radiation performance of the SMRS antenna, and the omnidirectional radiation characteristic from the azimuth direction can be clearly observed from the three-dimensional (3D) radiation pattern shown in Fig. 5a. The two-dimensional (2D) normalized radiation patterns in $\varphi = 0°$ and $\varphi = 90°$ planes at 30 GHz are demonstrated in Fig. 5b. Both of them show the main radiation lobe directs at 30° which exactly equals to the angle of the theoretical design with a 15 dB gain. Furthermore, it can be seen from Fig. 6a and b that the major lobe of the SMRS bulleye antenna can be scanned from 14° to 58° as the operating frequency sweeps from 28 to

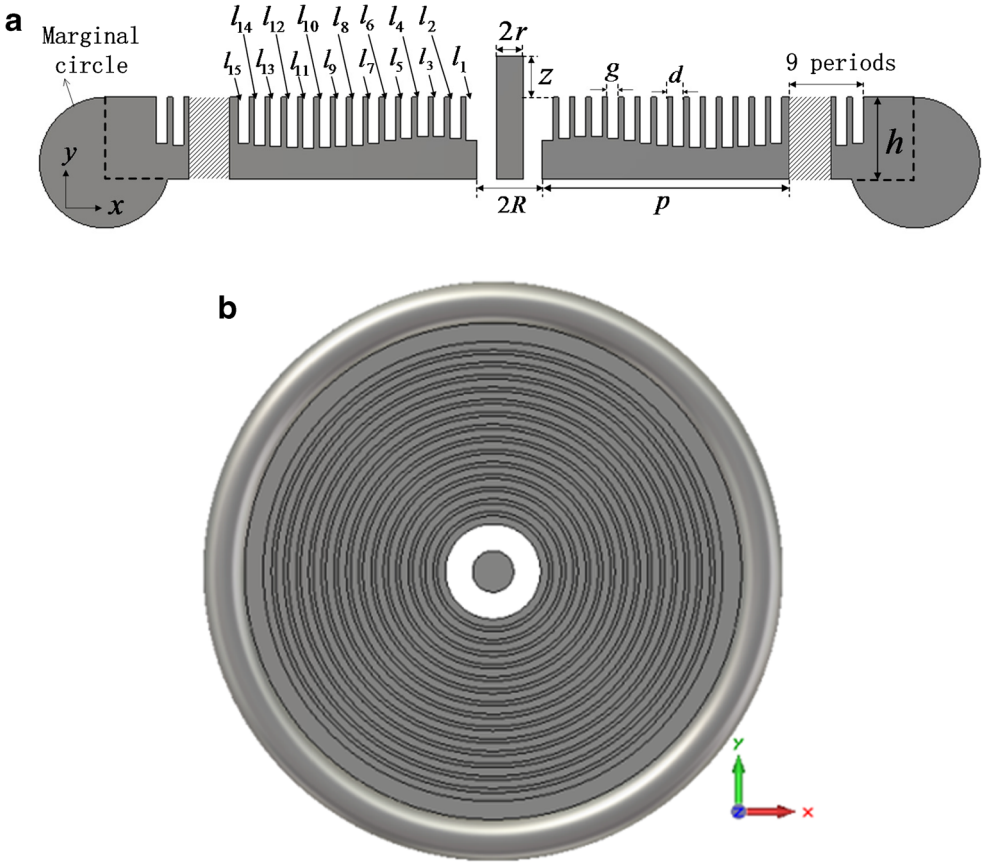

Fig. 2 Geometry of the proposed SMRS bulleye antenna. **a** Cross-section view. **b** Top view

32 GHz while the non-SMRS bulleye antenna does not have the property of beam scanning. The radiation patterns in the two principle planes are almost the same owing to the symmetry of structure and excitation, so we only give the comparison in $\varphi = 0°$ plane. The radiation efficiency of the SMRS antenna is nearly more than 90% in the operating band as displayed in Fig. 7, demonstrating that the design of sinusoidal modulation based on the bulleye structure proposed in this paper can efficiently convert guided SSPPs to radiating modes.

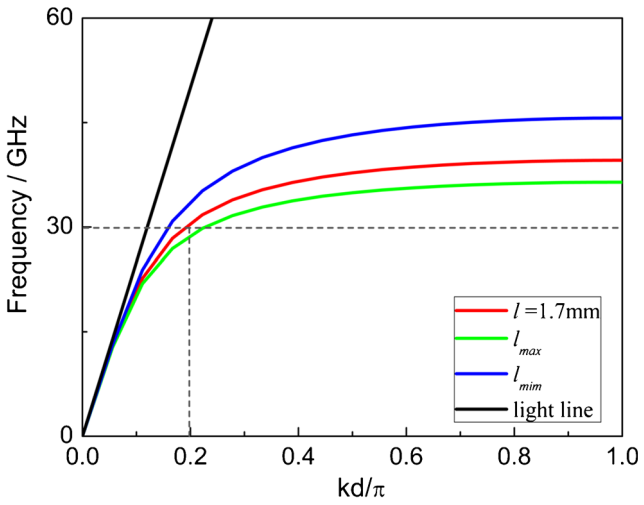

Fig. 3 Dispersion relations of SSPPs in corrugated structures with $d = 0.6$ mm, $g = 0.4$ mm, and $h = 4$ mm. The *black line* indicates the light line, the *red*, *blue*, and *green* line respectively represent numerical dispersion curves with different depth of grooves in which $l = 1.7$ mm, $l_{min} = 1.44762$ mm, and $l_{max} = 1.86325$

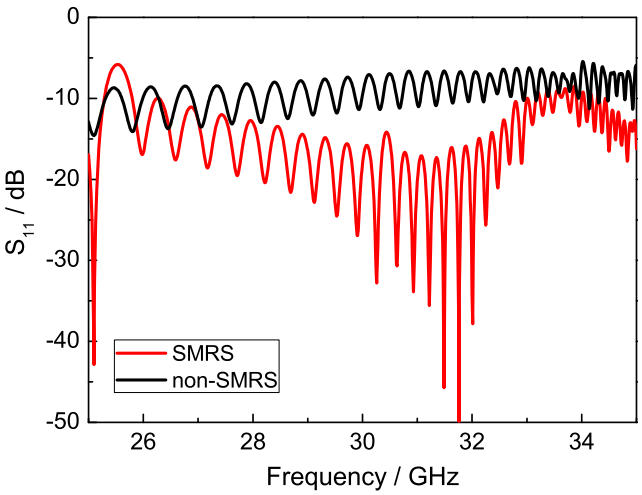

Fig. 4 Simulated reflection coefficient S_{11} of the proposed SMRS bulleye antenna and comparison with the non-SMRS bulleye antenna

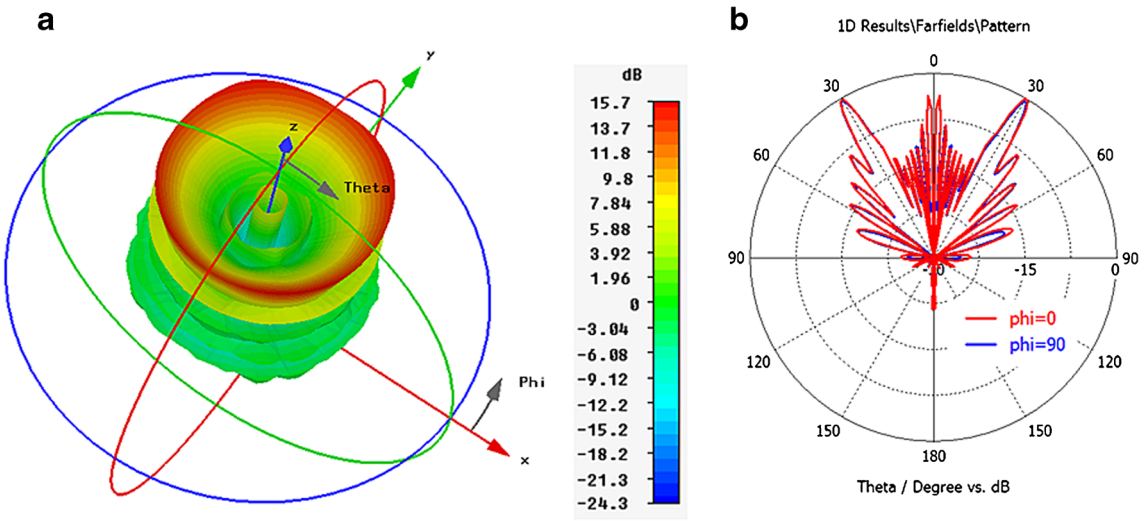

Fig. 5 Simulated far-field radiation properties of the proposed SMRS bulleye antenna. **a** 3D radiation patterns at 30 GHz. **b** Normalized 2D radiation patterns in $\phi = 0°$ and $\phi = 90°$ planes at 30 GHz

Fig. 6 Frequency scanning characteristic of SMRS and non-SMRS bulleye antenna. **a** Normalized 2D radiation patterns of SMRS bulleye antenna in $\phi = 0°$ plane at different frequencies. **b** Normalized 2D radiation patterns of non-SMRS bulleye antenna in $\phi = 0°$ plane at different frequencies

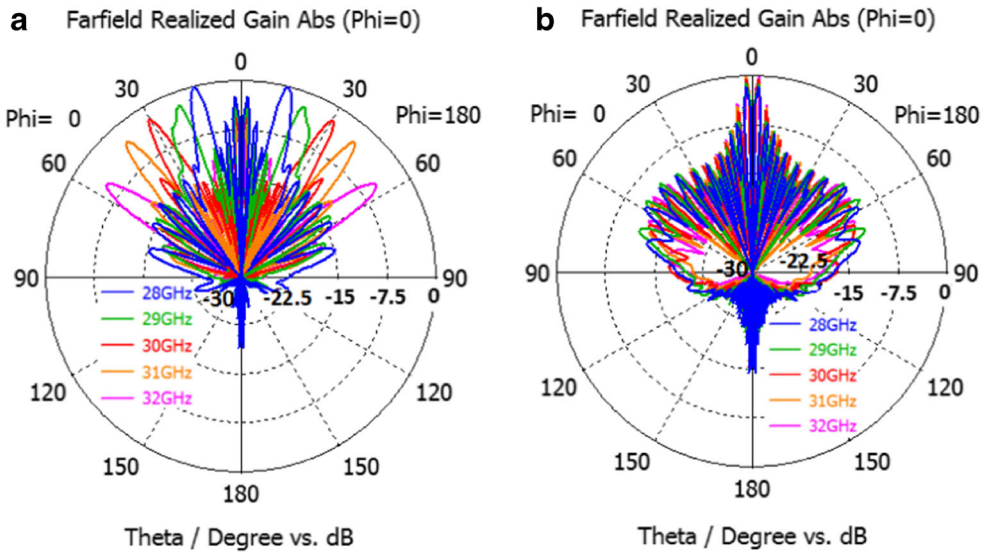

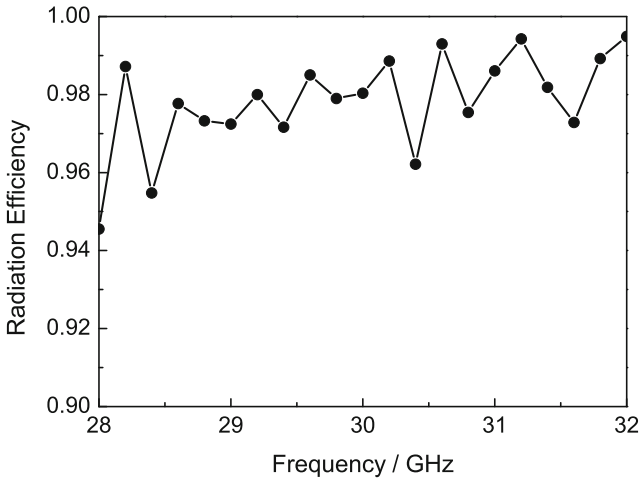

Fig. 7 Radiation efficiency of SMRS bulleye antenna

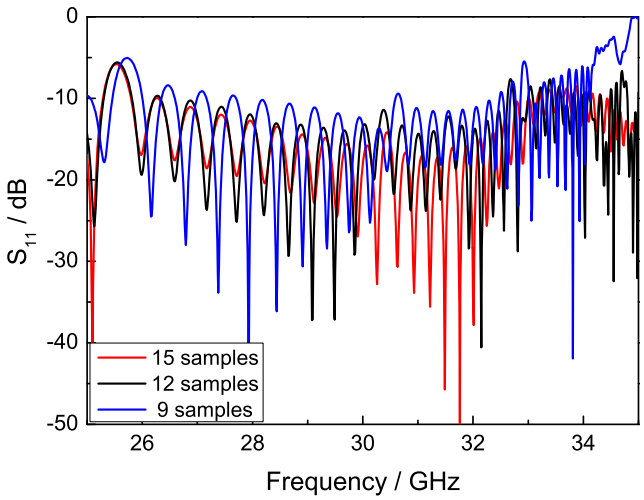

Fig. 8 Simulated reflection coefficient S_{11} of SMRS bulleye antenna with three different samples(15, 12, and 9) in one sinusoidal period

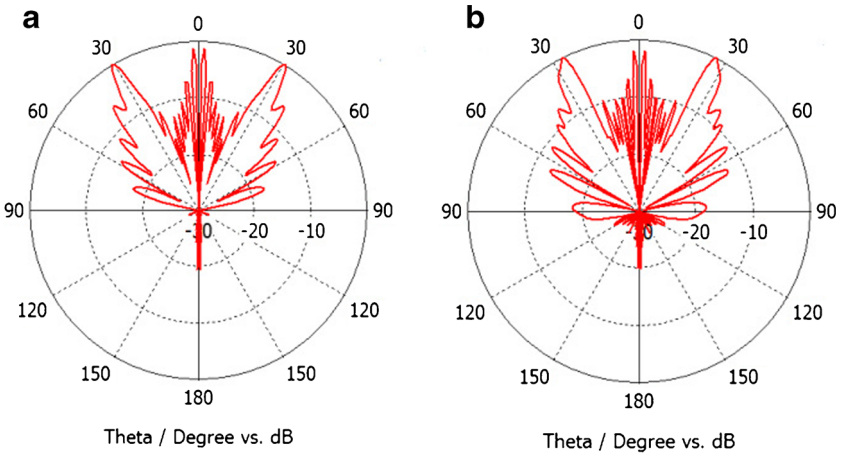

Fig. 9 Normalized 2D radiation patterns in $\phi = 0°$ plane at 30 GHz. **a** Twelve samples in a sinusoidal period. **b** Nine samples in a sinusoidal period

Moreover, in order to further demonstrate why 15 sub-unit-cells in one period are sufficient to mimic a continuous sinusoidal shape mentioned above, simulations are carried out on the designed bulleye structure with three different samples(15, 12, and 9) in one period to mimic a continuous sinusoidal shape and the reflection coefficients of these three different structures are compared in Fig. 8. Figure 9 shows that the main radiation lobe directs at 31° and 27° respectively for 12 and 9 samples in one sinusoidal period. It is concluded that the reflection coefficient S_{11} is getting better and the main radiation lobe directs more accurately at the designed angle with increase of the discrete sample numbers from the simulated results. The main radiation lobe can direct just at 30° which is the angle of the theoretical design when we use 15 samples. Thus no more samples are required and 15 sub-unit-cells in one period are sufficient to mimic a continuous sinusoidal shape.

Conclusions

In summary, a new bulleye antenna which can convert guided spoof plasmons to radiating modes is proposed in this paper. It essentially relies on the effective mapping of a sinusoidal impedance variation to a sinusoidal groove depth variation. The main direction and beamwidth of radiation lobe in the elevation plane is determined by the modulation parameters and the radiation pattern is omnidirectional in azimuth plane. Besides, the designed antenna has a wide operating bandwidth of 7.2 GHz and it is easy to realize beam scanning by tuning the working frequency. The radiation efficiency of the bulleye antenna is nearly more than 90% in the whole operating band, which can find potential applications in transmitting and receiving electromagnetic waves in the specific direction in SSPPs system.

Acknowledgments This work was supported in part by the Fundamental Research Funds for the Central Universities under Grant No. NS2016039, the Foundation of State Key Laboratory of Millimeter Waves, Southeast University, China, under Grant No. K201603, the Natural Science Foundation of Jiangsu Province under Grant No. BK20151480, and the priority academic program development of Jiangsu Higher Education Institutions.

References

1. Maier SA (2007) Plasmonics:fundamentals and applications Springer Science & Business Media
2. Barnes WL, Dereux A, Ebbesen TW (2003) Surface plasmon subwavelength optics. Nature 424:824–830
3. Novotny L, Hecht B (2012) Principles of nano-optics Cambridge university press
4. Verhagen E, Polman A, Kuipers LK (2008) Nanofocusing in laterally tapered plasmonic waveguides. Opt Express 16:45–57
5. Stewart ME, Anderton CR, Thompson LB et al. (2008) Nanostructured plasmonic sensors. Chem Rev 108:494–521
6. Pendry JB, Martin-Moreno L, Garcia-Vidal FJ (2004) Mimicking surface plasmons with structured surfaces. Science 305:847–848
7. Maier SA, Andrews SR, Martin-Moreno L et al. (2006) Terahertz surface plasmon-polariton propagation and focusing on periodically corrugated metal wires. Phys Rev Lett 97:176805
8. De Abajo FJG, Senz JJ (2005) Electromagnetic surface modes in structured perfect-conductor surfaces. Phys Rev Lett 95:233901
9. Fernandez-Dominguez AI, Martin-Moreno L, Garcia-Vidal FJ et al. (2008) Spoof surface plasmon polariton modes propagating along periodically corrugated wires. IEEE J Sel Top Quantum Electron 14:1515–1521
10. Ma HF, Shen X, Cheng Q et al. (2014) Broadband and high-efficiency conversion from guided waves to spoof surface plasmon polaritons. Laser Photonics Rev 8:146–151
11. Liu L, Li Z, Gu C et al. (2015) Smooth bridge between guided waves and spoof surface plasmon polaritons. Opt Lett 40:1810–1813
12. Yin JY, Ren J, Zhang HC et al. (2015) Broadband frequency-selective spoof surface plasmon polaritons on ultrathin metallic structure. Sci Report 5:8165

13. Xu J, Li Z, Liu L et al. (2016) Low-pass plasmonic filter and its miniaturization based on spoof surface plasmon polaritons. Opt Commun 372:155–159
14. Shibayama J, Yamauchi J, Nakano H (2015) Metal disc-type splitter with radially placed gratings for terahertz surface waves. Electron Lett 51:352–353
15. Oliner AA, Jackson DR, Volakis JL (2007) Antenna engineering handbook McGraw Hill
16. Yin JY, Zhang HC, Fan Y et al. (2016) Direct radiations of surface plasmon polariton waves by gradient groove depth and flaring metal structure. IEEE Antennas Wirel Propag Lett 15:865–868
17. Xu JJ, Zhang HC, Zhang Q et al. (2015) Efficient conversion of surface-plasmon-like modes to spatial radiated modes. Appl Phys Lett 106:021102
18. Oliner A, Hessel A (1959) Guided waves on sinusoidally-modulated reactance surfaces. IRE Trans Anntenas Propag 7:201–208
19. Panaretos AH, Werner DH (2016) Spoof plasmon radiation using sinusoidally modulated corrugated reactance surfaces. Opt Express 24:2443–2456
20. Kong GS, Ma HF (2015) Omnidirectional antenna based on modulated spoof surface plasmon polaritons waveguide, 2015 Asia-Pacific Microwave Conference (APMC). IEEE 3:1–3
21. Monnai Y, Jahn D, Withayachumnankul W et al. (2015) Terahertz plasmonic Bessel beamformer. Appl Phys Lett 106:021101
22. Ishimaru A (2015) A, Electromagnetic wave propagation, radiation, and scattering Prentice-Hall
23. Harrington RF (2001) Time-Harmonic Electromagnetic Fields, Wiley-IEEE